Research Article

Magnetic Resonance in Chemistry

Received: 4 September 2007 Revised: 1 October 2007 Accepted: 1 October 2007 Published online in Wiley Interscience:

(www.interscience.com) DOI 10.1002/mrc.2116

Origin of ^{13}C complexation shifts in the adduct formation of 2-butyl phenyl ethers with a dirhodium tetracarboxylate complex

Edison Díaz Gómez and Helmut Duddeck*

Complexation of the oxygen atom in 2-butyl phenyl ethers to a rhodium atom of the dirhodium tetracarboxylate $Rh^{(II)}_2$[(*R*)-(+)-MTPA]$_4$(Rh*, MTPA-H = methoxytrifluoromethylphenylacetic acid ≡ Mosher's acid) deshields an sp^3-hybridized ^{13}C nucleus directly bonded to the ether oxygen; apparently, the inductive effect of the oxygen is enhanced when it is complexed to the rhodium atom. On the other hand, deshielding complexation shifts of aromatic *ipso*-carbons (α-positioned) are minute but *ortho*- and *para*-carbon signals are influenced by the resonance effect of oxygen. This effect can be modulated by further substituents at the benzene ring. In turn, this modulation of the resonance correlates linearly ith the magnitude of the inductive effect exerted on the aliphatic α–carbon atoms. Diastereomeric dispersion effects at ^{13}C signals can be observed for most compounds, indicating that enantiodifferentiation is possible in this class of ethers.

Keywords: 2-butyl phenyl ethers; dirhodium complexes; complexation; ^{13}C NMR; ^{1}H NMR; inductive effect; resonance effect; chiral differentiation

Introduction

Dirhodium complexes as well as their adducts are in the focus of interest for many years.[1] They were introduced as homogeneous catalysts in various reactions[2] and have found even medicinal application.[3] During the last decade, we have shown that the enantiomers of many chiral ligands, particularly those of soft Lewis bases, can easily be differentiated by adding an equimolar amount of the dirhodium complex $Rh^{(II)}_2$[(*R*)-(+)-MTPA]$_4$ ([**Rh***], (MTPA-H) = methoxytrifluoromethylphenylacetic acid ≡ Mosher's acid; see Scheme 1) to their $CDCl_3$ solution and monitoring the diastereomeric dispersion $\Delta\nu$ of their ^{1}H (or ^{13}C) NMR signals at room temperature (dirhodium method).[4]

The complexation site of the ligand molecule can be determined by moderate deshieldings of nearby ^{1}H and – particularly – ^{13}C nuclei (complexation shifts $\Delta\delta$). In a qualitative interpretation of positive $\Delta\delta$ values, one can assume an increase of the electron-acceptor properties of the atom which is the binding site (inductive effect).[4] Recently, however, when investigating oxygen ligands which were attached to aromatic ring systems, we encountered the observation that significant complexation shifts may be found on aromatic atoms beyond the *ipso*-carbon bound to oxygen. For example, complexation shifts in cyclotriveratrylenes containing three methoxy groups (Scheme 2) are much stronger at the two *ortho*- and the at the *para*-carbon atoms than at the methoxylated carbon.[5] This, however, is not compatible with an explanation based on an inductive effect of the oxygen but rather reminds of a resonance effect.

So, we decided to conduct a more detailed study on this phenomenon, i.e. the fact that complexations shifts seem to be entirely different if aliphatic or aromatic carbons are involved. Ethers were chosen as suitable candidates because – as hard Lewis bases – they form rather weak adducts with **Rh***.[4] The binding energy is expected to be based primarily on electrostatic interaction; orbital interaction (HOMO-LUMO) should not contribute significantly if oxygen as a second-row element is involved; the HOMO-LUMO gap is too large.[6] We chose the 2-butyl group as the aliphatic part and the phenyl group as the aromatic residue, both attached to oxygen. The chiral 2-butyl group (in racemic form) offers carbon-hydrogen fragments of different compositions, and their ^{1}H and ^{13}C signals are easy to identify. Moreover, the chirality allows monitoring the potential for enantiodifferentiation in these ethers, in addition. On the other hand, the electronic interaction inside the phenyl group can easily be modulated by attaching substituents X. Thus, a series of 2-butyl phenyl ethers (Scheme 3) were subjected to the dirhodium experiment.

Experimental

Substances

The synthesis of **Rh*** has been described by us earlier.[7]

The 2-butyl phenyl ethers **1**–**5d** were prepared as racemates by a nucleophilic substitution reaction of 2-bromobutane and the respective phenolates (Williamson's ether synthesis). General procedure: 20 mmol K_2CO_3 (2.76 g) was suspended in 20 ml acetone, and then 22 mmol 2-iodobutane (4.0 g, 2.5 ml) was added followed by 20 mmol of the respective, commercially available phenol. The mixture was refluxed under stirring for 48 h, acetone distilled off with a rotary evaporator and the residue poured into 20 ml water. The aqueous layer was extracted twice with 2 ml

* *Correspondence to: Helmut Duddeck, Leibniz University Hannover, Institute of Organic Chemistry, Schneiderberg 1B, D-30167 Hannover, Germany. E-mail: duddeck@mbox.oci.uni-hannover.de*

Leibniz University Hannover, Institute of Organic Chemistry, Schneiderberg 1B, D-30167 Hannover, Germany

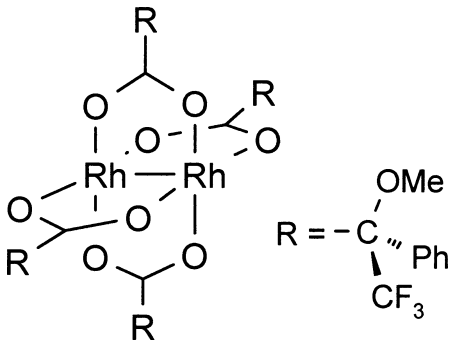

Scheme 1. Structure of the dirhodium complex **Rh***.

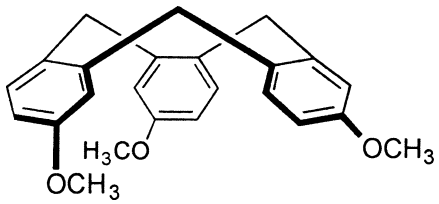

Scheme 2. Structure of a cyclotriveratrylene derivative containing three methoxy groups.

toluene, and the combined organic layers were washed twice with aqueous sodium hydroxide (10%) and with water. After removal of the solvent, the crude product was distilled *in vacuo*. The ethers were obtained as colorless or slightly yellow liquids; yields were 60–75% (not optimized). Purification by chromatography on silica gel should be avoided because it leads to massive losses probably due to a H^+-catalyzed phenol elimination.

Most of the ethers, namely **1**,[8] **2a**,[9] **2b**,[10] **2c**,[11] **2d**,[12] **2e**,[13] **3a**,[9] **3b**,[14] **3c**,[15] and **5d**,[16] are described in the literature; **3d, 4c** and **5c** are new. In nearly all cases, spectral data are not well documented in the literature. Therefore, we collect here ^{1}H NMR chemical shifts, infrared and electron-impact mass spectral data of all derivatives. IR spectra were recorded on a Bruker Vector 22 spectrometer and EI-MS spectra on a Micromass LCT instrument.

*2-Butyl phenyl ether, (1-methylpropoxy)benzene (**1**)*

^{1}H chemical shifts δ (ppm), signal multiplicities m and complexation shifts $\Delta\delta$ (in parentheses), in $CDCl_3$: H-1, 1.29, d (+0.02); H-2, 4.29, tq (+0.03); H-3a, 1.61, ddq (+0.01); H-3b, 1.75, ddq (+0.03); H-4, 0.97, t (+0.01); H-2′/6′, 6.89, m (+0.03); H-3′/5′, 7.26, m (+0.01); H-4′, 6.90, m (+0.04). IR (liquid) $\tilde{\nu}$ (cm^{-1}) 2971, 2934, 1598, 1586, 1492, 1290, 1239, 923, 749, 691. EI-MS (70 eV, rel. int. %) *m/z* 150 (19, M^+), 121 (20), 95 (12), 94 (100), 77 (15), 66 (13), 65 (10).

*1-Fluoro-4(1-methylpropoxy)benzene (**2a**)*

^{1}H chemical shifts δ (ppm), signal multiplicities m and complexation shifts $\Delta\delta$ (in parentheses), in $CDCl_3$: H-1, 1.27, d (+0.04); H-2, 4.19, tq (+0.06); H-3a, 1.60, ddq (+0.01); H-3b, 1.73, ddq (+0.05); H-4, 0.97, t (+0.01); H-2′/6′, 6.82, m (+0.06); H-3′/5′, 6.95, m (−0.01); IR (liquid) $\tilde{\nu}$ (cm^{-1}) 2973, 2935, 2880, 1600, 1501, 1378, 1245, 1205, 1104, 825, 746, 730. EI-MS (70 eV, rel. int. %) *m/z* 168 (13, M^+), 139 (6), 112 (100), 95 (9), 83 (12), 75 (7), 57 (13).

*1-Chloro-4(1-methylpropoxy)benzene (**2b**)*

^{1}H chemical shifts δ (ppm), signal multiplicities m and complexation shifts $\Delta\delta$ (in parentheses), in $CDCl_3$: H-1, 1.27, d (0); H-2, 4.24, tq (+0.03); H-3a, 1.60, ddq (+0.01); H-3b, 1.73, ddq (0); H-4, 0.96, t (+0.01); H-2′/6′, 6.81, m (+0.03); H-3′/5′, 7.21, m (0); IR (liquid) $\tilde{\nu}$ (cm^{-1}) 2973, 2935, 1595, 1579, 1487, 1378, 1238, 1091, 823, 664. EI-MS (70 eV, rel. int. %) *m/z* 184/186 (10/3, M^+), 128/130 (100/31), 111/113 (6/2), 100/102 (4/1), 99/101 (13/4), 65 (9).

*1-Bromo-4(1-methylpropoxy)benzene (**2c**)*

^{1}H chemical shifts δ (ppm), signal multiplicities m and complexation shifts $\Delta\delta$ (in parentheses), in $CDCl_3$: H-1, 1.27, d (+0.02); H-2, 4.24, tq (+0.03); H-3a, 1.60, ddq (+0.01); H-3b, 1.73, ddq (+0.03); H-4, 0.96, t (0); H-2′/6′, 6.77, m (+0.02); H-3′/5′, 7,35, m (0); IR (liquid) $\tilde{\nu}$ (cm^{-1}) 2972, 2934, 2878, 1589, 1485, 1282, 1237, 1072, 820. EI-MS (70 eV, rel. int. %) *m/z* 228/230 (11/11, M^+), 172/174 (100/93), 143/145 (9/9), 93 (14), 75 (7), 65 (16), 63 (14), 57 (8).

*1-Iodo-4(1-methylpropoxy)benzene (**2d**)*

^{1}H chemical shifts δ (ppm), signal multiplicities m and complexation shifts $\Delta\delta$ (in parentheses), in $CDCl_3$: H-1, 1.27, d (0); H-2, 4.24,

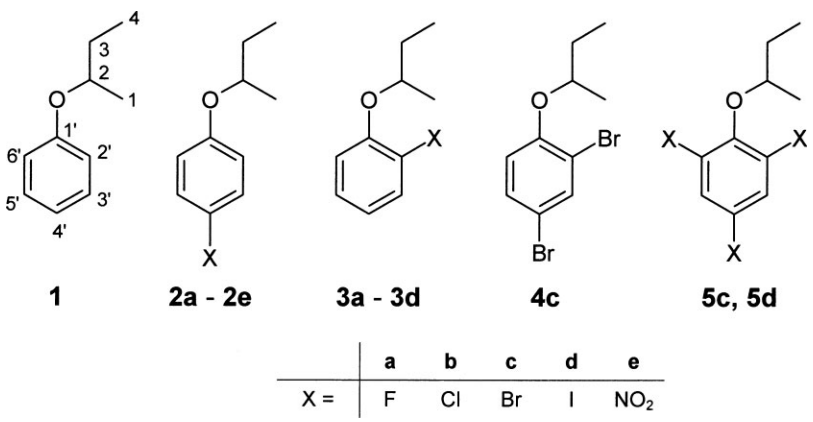

Scheme 3. Structures of the 2-butyl phenyl ethers studied.(The nomenclature and atom numbering of the substituted 2-butyl phenyl ethers differs from that of the unsubstituted **1**; e.g. **2a** is 1-flouro-4(1-methylpropoxy)benzene. For a better comparability of NMR data, however, we used the atom numbering of **1** for all derivatives **2a to 5d**.

tq (−0.01); H-3a, 1.60, ddq (−0.01); H-3b, 1.72, ddq (+0.01); H-4, 0.96, t (−0.01); H-2′/6′, 6.66, m (−0.03); H-3′/5′, 7.53, m (+0.04); IR (liquid) $\tilde{\nu}$ (cm^{-1}) 2971, 2932, 2877, 1583, 1482, 1279, 1237, 998, 818. EI-MS (70 eV, rel. int. %) *m/z* 276 (23, M^+), 220 (100), 112 (39), 93 (27), 76 (10), 65 (23), 57 (9).

*1-Nitro-4(1-methylpropoxy)benzene (**2e**)*

^1H chemical shifts δ (ppm), signal multiplicities m and complexation shifts $\Delta\delta$ (in parentheses), in $CDCl_3$: H-1, 1.34, d (0); H-2, 4.43, tq (0); H-3a, 1.68, ddq (0); H-3b, 1.79, ddq (0); H-4, 0.99, t (0); H-2′/6′, 6.92, m (0); H-3′/5′, 8.18, m (+0.01); IR (liquid) $\tilde{\nu}$ (cm^{-1}) 2974, 2936, 1591, 1509, 1493, 1338, 1255, 1177, 1108, 920, 844, 752, 691. EI-MS (70 eV, rel. int. %) *m/z* 195 (29, M^+), 166 (10), 140 (100), 139 (86), 123 (31), 109 (100), 93 (26), 81 (19), 76 (22), 65 (44).

*1-Fluoro-2(1-methylpropoxy)benzene (**3a**)*

^1H chemical shifts δ (ppm), signal multiplicities m and complexation shifts $\Delta\delta$ (in parentheses), in $CDCl_3$: H-1, 1.31, d (+0.06); H-2, 4.28, tq (+0.09); H-3a, 1.64, ddq (+0.04); H-3b, 1.80, ddq (+0.09); H-4, 1.00, t (0); H-3′, 7.06, m (0.0), H-4′, 6.88, m (+0.06); H-5′, 7.03, m (+0.03); H-6′, 6.97, m (+0.07). IR (liquid) $\tilde{\nu}$ (cm^{-1}) 2973, 2936, 2879, 1612, 1501, 1457, 1257, 1110, 744. EI-MS (70 eV, rel. int. %) *m/z* 168 (7, M^+), 139 (13), 121 (6), 112 (100), 94 (26), 83 (9), 64 (12), 57 (12).

*1-Chloro-2(1-methylpropoxy)benzene (**3b**)*

^1H chemical shifts δ (ppm), signal multiplicities m and complexation shifts $\Delta\delta$ (in parentheses), in $CDCl_3$: H-1, 1.33, d (0); H-2, 4.32, tq (+0.01); H-3a, 1.67, ddq (+0.01); H-3b, 1.80, ddq (+0.02); H-4, 1.01, t (0); H-3′, 7.35, m (+0.01), H-4′, 6.86, m (+0.02); H-5′, 7.18, m (+0.01); H-6′, 6.93, m (+0.02). IR (liquid) $\tilde{\nu}$ (cm^{-1}) 2973, 2936, 2879, 1612, 1501, 1457, 1257, 1110, 744.IR (liquid) (cm^{-1}) 2973, 2935, 2878, 1588, 1478, 1445, 1378, 1273, 1245, 1059, 924, 744, 690. EI-MS (70 eV, rel. int. %) *m/z* 184/186 (6/2, M^+), 128/130 (100/34), 112 (7), 92 (6), 75 (6), 64 (9).

*1-Bromo-2(1-methylpropoxy)benzene (**3c**)*

^1H chemical shifts δ (ppm), signal multiplicities m and complexation shifts $\Delta\delta$ (in parentheses), in $CDCl_3$: H-1, 1.33, d (0); H-2, 4.33, tq (+0.01); H-3a, 1.68, ddq (+0.01); H-3b, 1.80, ddq (+0.02); H-4, 1.01, t (0); H-3′, 7.53, m (+0.01), H-4′, 6.80, m (+0.01); H-5′, 7.22, m (+0.01); H-6′, 6.90, m (+0.02). IR (liquid) $\tilde{\nu}$ (cm^{-1}) 2973, 2936, 2879, 1612, 1501, 1457, 1257, 1110, 744.IR (liquid) (cm^{-1}) 2972, 2934, 2878, 1585, 1474, 1441, 1378, 1272, 1244, 1029, 924, 743, 663. EI-MS (70 eV, rel. int. %) *m/z* 228/230 (8/7, M^+), 172/174 (100/95), 143/145 (9/8), 92/94 (5/5), 63 (16), 57 (10).

*1-Iodo-2(1-methylpropoxy)benzene (**3d**)*

^1H chemical shifts δ (ppm), signal multiplicities m and complexation shifts $\Delta\delta$ (in parentheses), in $CDCl_3$: H-1, 1.34, d (0); H-2, 4.35, tq (+0.01); H-3a, 1.69, ddq (+0.01); H-3b, 1.79, ddq (+0.01); H-4, 1.02, t (−0.01); H-3′, 7.77, m (+0.05), H-4′, 6.67, m (−0.06); H-5′, 7.26, m (0); H-6′, 6.80, m (+0.01). IR (liquid) $\tilde{\nu}$ (cm^{-1}) 2973, 2936, 2879, 1612, 1501, 1457, 1257, 1110, 744. IR (liquid) (cm^{-1}) 2971, 2932, 2876, 1580, 1467, 1270, 1243, 1126, 1016, 923, 743. EI-MS (70 eV, rel. int. %) *m/z* 276 (18, M^+), 220 (100), 112 (20), 93 (16), 76 (7), 65 (20).

*1,3-Dibromo-6(1-methylpropoxy)benzene (**4c**)*

^1H chemical shifts δ (ppm), signal multiplicities m and complexation shifts $\Delta\delta$ (in parentheses), in $CDCl_3$: H-1, 1.32, d (+0.01); H-2, 4.29, tq (0); H-3a, 1.67, ddq (+0.01); H-3b, 1.78, ddq (+0.02); H-4, 1.00, t (0); H-3′, 7.66, dd (+0.01), H-5′, 7.33, dd (0); H-6′, 6.76, d (+0.01). IR (liquid) $\tilde{\nu}$ (cm^{-1}) 2972, 2933, 2878, 1577, 1467, 1379, 1282, 1260, 1243, 1094, 1042, 801, 690. EI-MS (70 eV, rel. int. %) *m/z* 306/308/310 (4/8/4, M^+), 250/252/254 (55/100/56), 221/223/225 (4/6/4), 128 (12), 63 (15), 57 (8).

*1,3,5-Tribromo-6(1-methylpropoxy)benzene (**5c**)*

^1H chemical shifts δ (ppm), signal multiplicities m and complexation shifts $\Delta\delta$ (in parentheses), in $CDCl_3$: H-1, 1.28, d (0); H-2, 4.54, tq (0); H-3a, 1.72, ddq (0); H-3b, 1.85, ddq (0); H-4, 1.00, t (0); H-3′/5′, 7.65, s (0). IR (liquid) $\tilde{\nu}$ (cm^{-1}) 2968, 2934, 2876, 1559, 1535, 1436, 1372, 1246, 1088, 899, 857, 739, 727. EI-MS (70 eV, rel. int. %) *m/z* 384/386/388/390 (1/2/2/1, M^+), 369/371/373/375 (0.5/1/1/0.5), 355/357/359/361 (2/4/4/2), 328/330/332/334 (41/100/98/38), 229/301/303/305 (3/6/6/3), 248/250/252/254 (3/6/6/3), 143 (13), 141 (13), 74 (6), 62 (16), 57 (12).

*1,3,5-Triiodo-6(1-methylpropoxy)benzene (**5d**)*

^1H chemical shifts δ (ppm), signal multiplicities m and complexation shifts $\Delta\delta$ (in parentheses), in $CDCl_3$: H-1, 1.30, d (−0.01); H-2, 4.62, tq (0); H-3a, 1.76, ddq (0); H-3b, 1.88, ddq (−0.01); H-4, 1.00, t (−0.01); H-3′/5′, 8.06, s (+0.02). IR (liquid) $\tilde{\nu}$ (cm^{-1}) 2964, 2930, 1517, 1413, 1377, 1238, 1085, 895, 859, 721, 693. EI-MS (70 eV, rel. int. %) *m/z* 528 (8, M^+), 472 (100), 346 (49), 218 (27), 189 (20), 127 (5), 91 (10), 62 (26).

NMR spectroscopy

Room-temperature ^1H (400.1 MHz) and ^{13}C (100.6 MHz) NMR measurements were performed on a Bruker Avance DPX-400 spectrometer. Samples were *ca* 0.01–0.025 mmolar in $CDCl_3$. Chemical shift standard was internal tetramethylsilane ($\delta = 0$).

Following parameters have been used for all one-dimensional NMR spectra. ^1H: acquisition time 4.0 s, relaxation delay 0.5 s, pulse duration 2.6 μs for a 30° flip angle, and spectral width 8224 Hz (20.6 ppm); 64K points were used for data acquisition, 64K points for FT transformation and digital resolution was 0.12 Hz/point. ^{13}C: acquisition time 2.6 s for a 30° flip angle, relaxation delay 0.5 s, pulse duration 2.3 μs, and spectral width 25.629 Hz (250 ppm); 128K points were used for data acquisition, 128K points for FT transformation and digital resolution was 0.19 Hz/point.

Signal assignments were assisted by DEPT90 and DEPT135, COSY, HMQC and HMBC spectra (standard Bruker software and parameters):

Gradient-selected ^1H, ^1H COSY spectra: relaxation delay $D_1 = 1.2$ s; 90° pulse for ^1H: 9.6 μs; 1024 points in t_2; 256 experiments in t_1, linear prediction to 512 points, zero-filling up to 1K.

Gradient-selected HMQC spectra: relaxation delay $D_1 = 1.5$ s, evolution delay $D_2 = 3.45$ ms, 90° pulse: 9.6 μs for ^1H, 12.1 μs for ^{13}C hard pulses and 66.0 μs for ^{13}C GARP decoupling; 1K points in t_2; 256 experiments in t_1, linear prediction to 512 and zero-filling up to 1K.

Gradient-selected HMBC spectra: relaxation delay $D_1 = 1.5$ s; evolution delay $D_2 = 3.45$ ms; 90° pulse: 9.6 μs for ^1H, 12.1 μs for ^{13}C hard pulses, delay for evolution of long-range coupling

$D_6 = 70$ ms ($J = 7$ Hz); 1K points in t_2; 256 experiments in t_1, linear prediction to 512 and zero-filling up to 1K.

In the standard dirhodium experiment, **Rh*** and equimolar amounts of the ligands **1**–**5d**, respectively, were dissolved in 0.7 ml $CDCl_3$; quantities of 10–25 mg of **Rh*** (*ca* 0.01–0.025 mmolar concentration) were employed. If necessary, the dissolution process was accelerated by exposing the NMR sample tubes to an ultrasonic bath for a couple of minutes. In earlier reports on soft-base ligands, the use of acetone-d_6 for increasing the solubility of **Rh*** has been recommended.[4] This auxiliary, however, should be avoided when hard-base ligands such as ethers are involved because acetone-d_6 is a competitor in the adduct formation in such cases.

Note that $\Delta\nu$ values are B_0 dependent and have no signs here because racemates have been investigated. In this work, all dispersion values are given as integers in hertz as determined at $B_0 = 9.4$ T corresponding to 400 MHz ^{1}H and 100.6 MHz ^{13}C.

Results and Discussion

The complete and unambiguous NMR signal assignment of the free ligands **1**–**5d** (Scheme 3) is straightforward when routine NMR methods such as DEPT, COSY, HMQC and HMBC techniques are applied. For the ^{1}H chemical shifts see 'Experimental', and for ^{13}C see Table 1. In the case of **Rh*** adducts the identification of some ligand signals is hampered by overlapping Mosher acid signals when aromatic signals are involved.

^{13}C chemical shifts (δ) of the 2-butyl phenyl ethers 1–5d

All ^{13}C NMR signals of all free ligands **1**–**5d** are collected in the Table 1. It should be noted that the values in italics (for the aromatic carbons) were obtained from calculations using a simple additivity rule: increments for the substituents X have been extracted from the ^{13}C NMR spectra of the corresponding monosubstituted benzenes recorded under identical conditions. (These increments are not reported here because they are very close to those listed in a comprehensive review[17] and in standard spectroscopy textbooks.) As expected, most calculated values correspond well to the experimental ones (within ± 1 ppm). Exceptions (underlined italicized values) appear for the substituted carbons if there is at least one halogen in *ortho*-position with respect to oxygen; this is due to steric repulsion and, eventually, electronic through-space interaction between O and X. Two more exceptions are observed, e.g. for C-4′ in the *para*-F- and *para*-I derivatives **2a** and **2d**. Altogether, there is a good additivity for the unsubstituted carbons proving that the individual electronic properties of the alkoxy and the X substituents are not modified significantly by double substitution (OR and X). This additivity is the basis for the later discussion about how to identify the two mechanisms (induction and resonance) and about their interdependence.

If, however, three halogen atoms are introduced at the aromatic ring (**5c** and **5d**), two of them in *ortho*-position, severe nonadditivity effects occur (Table 1) but this is of no importance in the context of this study because both compounds do not show any change in their ^{1}H- and ^{13}C-chemical shifts and no measurable $\Delta\nu$ values. Apparently, a double *ortho*-substitution averts any approach of the oxygen atom to **Rh*** close enough for adduct formation. Therefore, these two compounds are ignored in the following.

^{13}C complexation shifts ($\Delta\delta$) of the 2-butyl phenyl ethers 1–4c

Although ethers are known to be weak ligands in an adduct formation equilibrium (Scheme 4; equilibrium constant $K \approx 1$),[4] significant complexation shifts $\Delta\delta$ [$\Delta\delta = \delta$(**Rh***-adduct) $- \delta$(free ligand)] and if the ether molecule is chiral, signal dispersions $\Delta\nu$ due to the existence of diastereomeric adducts can be observed under standard dirhodium method conditions (1 : 1 molar ratio of **Rh*** and the ligand).[5,18] As tested for **1**, other molar ratios, e.g. 2.5 : 1, afford practically the same NMR spectroscopic results. Apparently, the concentration of the adduct in the adduct formation equilibrium (Scheme 4) is – within certain

Table 1. ^{13}C chemical shifts (δ) of the 2-butyl phenyl ethers **1**–**5d** in ppm, recorded in $CDCl_3$. Values in italics are calculated by the incremental rule discussed in the text

C	1	2a[a]	2b	2c	2d	2e	3a[b]	3b	3c	3d	4c	5c	5d
1	19.26	19.19	19.12	19.10	19.09	18.93	19.31	19.26	19.22	19.19	19.08	19.09	19.24
2	74.92	76.09	75.52	75.42	75.26	75.94	77.48	77.00	76.92	76.76	77.34	81.93	82.10
3	29.19	29.12	29.07	29.05	29.05	28.93	29.19	29.26	29.15	29.16	29.05	29.45	29.55
4	9.80	9.75	9.72	9.72	9.71	9.57	9.73	9.70	9.69	9.77	9.61	9.85	10.02
1′	158.22	154.29	156.83	157.33	158.12	163.51	146.14	153.93	154.77	156.88	154.11	151.84	157.14
	–	*153.7*	*156.1*	*156.5*	*157.1*	*164.2*	*145.0*	*158.3*	*161.2*	*167.1*	*158.2*	*162.5*	*174.9*
2′	115.90	117.21	117.19	117.68	118.26	115.14	153.80	124.17	113.56	88.25	112.65	116.37	87.97
	–	*117.3*	*117.1*	*117.4*	*117.6*	*116.6*	*150.3*	*121.6*	*99.9*	*81.8*	*111.4*	*112.9*	*85.2*
3′	129.41	115.73	129.28	132.22	138.20	125.90	116.37	130.40	133.46	139.55	135.59	135.14	147.52
	–	*116.2*	*129.5*	*132.4*	*138.3*	*124.3*	*116.2*	*129.5*	*132.4*	*138.3*	*135.4*	*133.7*	*146.1*
4′	120.39	157.11	125.18	112.43	82.25	140.93	121.25	121.24	121.62	122.18	114.42	119.65	93.42
	–	*154.8*	*126.1*	*114.4*	*86.3*	*140.0*	*121.8*	*121.6*	*121.9*	*122.1*	*115.9*	*117.4*	*89.7*
5′	129.41	115.73	129.28	132.22	138.20	125.90	124.14	127.48	128.21	129.21	131.02	135.14	147.52
	–	*116.2*	*129.5*	*132.4*	*138.3*	*124.3*	*124.9*	*126.3*	*127.7*	*128.3*	*130.7*	*133.7*	*146.1*
6′	115.90	117.21	117.19	117.68	118.26	115.14	117.75	115.72	115.29	113.75	116.31	116.37	87.97
	–	*117.3*	*117.1*	*117.4*	*117.6*	*116.6*	*117.3*	*117.1*	*117.4*	*117.6*	*118.9*	*112.9*	*85.2*

[a] $^1J(^{19}F, ^{13}C) = 238.0$ Hz, $^2J(^{19}F, ^{13}C) = 22.9$ Hz, $^3J(^{19}F, ^{13}C) = 7.9$ Hz, $^4J(^{19}F, ^{13}C) = 2.2$ Hz.
[b] $^1J(^{19}F, ^{13}C) = 245.2$ Hz, $^2J(^{19}F, ^{13}C) = 18.8$ Hz (C-3′) and 10.5 (C-1′), $^3J(^{19}F, ^{13}C) = 7.1$ Hz (C-4′) and 3.8 (C-6′), $^4J(^{19}F, ^{13}C) = 2.1$ Hz.

Magnetic Resonance in Chemistry

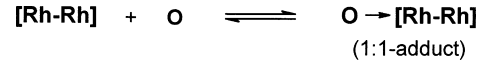

Scheme 4. Equilibrium between free components and the 1 : 1-adduct; **O** symbolizes the ether ligands **1**–**5d** and '**[Rh-Rh]**' the binuclear complex **Rh***.

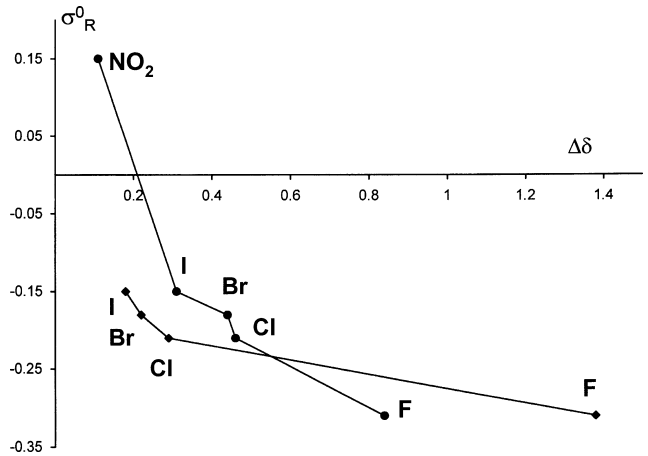

Figure 1. ^{13}C complexation shifts ($\Delta\delta$) of the atoms C-2′/6′ in the compounds **2a**–**2e** (•) and C-6′ in the compounds **3a**–**3d** (♦) (in ppm) plotted against the σ_R^0 parameters of the substituents X.

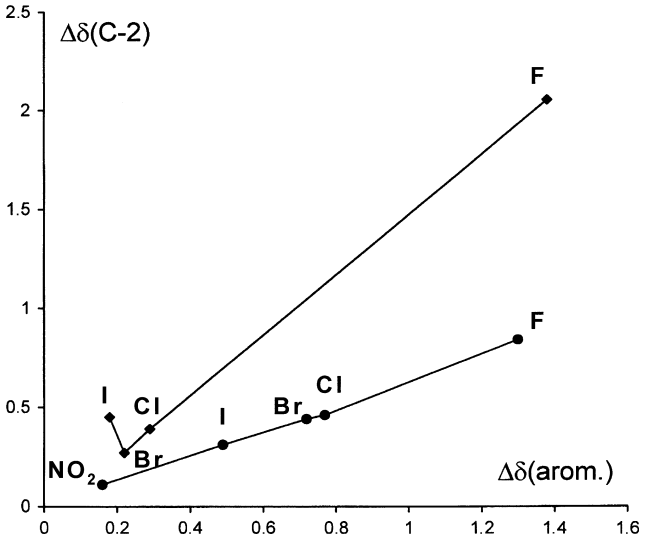

Figure 2. ^{13}C complexation shifts ($\Delta\delta$) of the aromatic carbon atoms C-2′/6′ in the compounds **2a**–**2e** (•) and C-6′ in the compounds **3a**–**3d** (♦) (in ppm) plotted against the ^{13}C complexation shifts of the aliphatic carbon atoms C-2 in the respective derivatives.

limits – independent of changes of the relative concentrations of the components. This proves that the equilibrium, indeed, contains a considerable amount of the free components and is not at all biased in favor of the adduct.

All $\Delta\delta(^{13}C)$ values obtained for the ethers **1**–**4c** are collected in Table 2; the data of the trihalo derivatives **5c** and **5d** have been omitted because their spectra give no indication of adduct formation. It is apparent that complexation shifts larger than +0.1 ppm appear at selected carbon atoms only. Among the aliphatic carbons, it is only C-2 which is affected ($\Delta\delta = +0.16 - +2.05$ ppm), whereas all others do not show any significant change. Obviously, this can be interpreted in terms of an increase of the electron-acceptor properties of oxygen by rhodium complexation but it is striking that substituents X at the aromatic ring have an influence as well: fluorine (**2a** and **3a**) enhances the group electronegativity considerably – and thereby the donor strength in the adduct – as compared to the unsubstituted parent compound **1**. The effects of chlorine and bromine substitution are small; iodine and the nitro group are even less effective, i.e. they weaken the donor property of oxygen as compared to **1**.

Unexpectedly, C-1′ nuclei, the oxygenated aromatic carbons, do no suffer significantly from electron-acceptor property changes of oxygen; all $\Delta\delta$-values are only between −0.15 (**2a**) and +0.14 (**2d**). On the other hand, carbons in *ortho*- and *para*-position with respect to oxygen are markedly deshielded by up to 1.38 ppm (**3a**), and – as for C-2 (see above) – there is a clear dependence on the nature of the substituents X. This evidence suggests that it is the resonance effect of X that modulates the complexation shifts of oxygen *via* the resonance properties of oxygen.

A great number of substituent parameters can be found in the literature to quantify such effects: Hammett σ constants, parameters from dual or even triple substituent parameter analyses and others.[19] The parameter σ_R^0 describing essentially the resonance properties of substituents attached to benzene is most suitable in the context of this study. Figure 1 shows that there is a fair correlation when the $\Delta\delta$ values of unsubstituted aromatic carbons in *ortho*-position to oxygen in the series **2a**–**3d** are plotted against the σ_R^0 values of X; the C-6′ value of **4c** with its two bromine atoms at C-2′ and C-4′ (+0.24 ppm) is very close to the respective one of the 2′-monobromo derivative **3c**.

Table 2. ^{13}C complexation shifts ($\Delta\delta$) of the 2-butyl phenyl ethers in ppm in the presence of an equimolar amount of **Rh***, recorded in $CDCl_3$

C	1	2a	2b	2c	2d	2e	3a	3b	3c	3d	4c
1	+0.02	+0.04	+0.02	+0.03	−0.02	+0.06	−0.05	−0.05	−0.04	−0.06	−0.03
2	+0.65	+1.30	+0.77	+0.72	+0.49	+0.16	+2.05	+0.39	+0.27	+0.45	+0.32
3	−0.02	−0.08	−0.04	−0.03	−0.05	+0.04	−0.14	−0.15	−0.04	−0.04	−0.04
4	+0.03	+0.09	+0.05	+0.04	+0.01	+0.05	+0.09	0.00	−0.01	−0.04	0.00
1′	+0.03	−0.15	−0.07	−0.03	+0.14	+0.07	−0.09	+0.05	+0.06	−0.05	+0.04
2′	+0.42	+0.84	+0.46	+0.44	+0.31	+0.11	+0.45	+0.14	+0.12	+0.45	+0.10
3′	+0.05	−0.03	−0.01	+0.01	−0.05	+0.10	+0.15	+0.04	+0.06	+0.01	+0.01
4′	+0.04	+0.27	+0.27	+0.28	+0.53	+0.10	+0.50	+0.04	+0.02	+0.07	+0.10
5′	+0.05	−0.03	−0.01	+0.01	−0.05	+0.10	−0.08	−0.01	+0.01	+0.19	+0.02
6′	+0.42	+0.84	+0.46	+0.44	+0.31	+0.11	+1.38	+0.29	+0.22	+0.18	+0.24

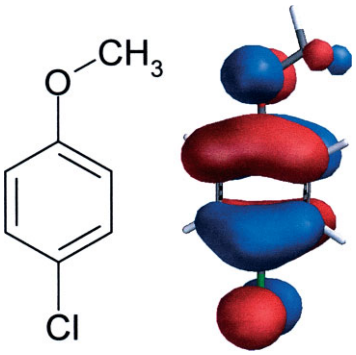

Figure 3. HOMO of the *O*-methyl analogue of **2c** calculated by density functional methods (B3LYP 6–31G*) using the SPARTAN '06 package, version 1.1.0.[20].

This indicates that, indeed, the resonance effect of oxygen dominates its complexations shifts in *ortho*- and *para*-positions, and this effect is modulated by resonance effects of substituents X attached to these carbons. Moreover, the extent of this resonance modulation, exerted from X on O, is transferred to the inductive effects of oxygen onto the directly bonded C-2. Figure 2 shows an excellent correlation for the *para*-substituted ethers of the series **2a**–**2e**; the correlation of the series **3a**–**3d** is not as good but still satisfactory.

Other aromatic carbon atoms substituted by X, e.g. C-4′ of **2a**–**2e** or C-2′ of **3,** show similar tendencies but the correlations are much less clear.

As a conclusion, one can deduce from these results that complexation shifts of oxygen ligands, produced by adduct formation with dirhodium complexes such as **Rh***, are essentially inductive in nature if directly attached aliphatic carbons are involved. In contrast, it is the resonance effect that rules the complexation shifts in the aromatic part of the ethers. Both mechanisms are not independent; there is an influence of the resonance effect on the inductive one via the intervening oxygen atom. Such interaction is plausible; consider that the HOMOs of *para*-substituted alkyl phenyl ethers, as shown in Fig. 3 for the *O*-methyl analogue of **2c**, are extended from the n_π-orbital of O to the n_π-orbital of X.[20] Remember that the HOMO-LUMO gap is dominating the mean excitation energy in the expression describing the paramagnetic term σ_p of the ^{13}C nuclear shielding.[21]

We are interested to see whether analogous relations exist for atoms other than oxygen when they act as binding sites to rhodium. Further studies to investigate soft Lewis-base atoms, as for example sulfur or selenium binding much stronger than oxygen and involving HOMO-LUMO interaction in the complexation, are currently in progress in our laboratory.

Enantiodifferentiation by ^{13}C and ^{1}H signal dispersion ($\Delta\nu$)

Although the ethers are weak ligands in their ability to bind to dirhodium tetracarboxylates,[5,18] some ^{13}C signal splittings can be observed for C-2 ($\Delta\nu = 3–6$ Hz) and C-2′/6′ ($\Delta\nu = 1–3$ Hz) of **1** and **2a**–**2d** due to the formation of diastereomeric adducts with **Rh***, respectively. If, however, the substituent is in *ortho*-position (**3a**–**3d**), diastereomeric dispersion effects are significantly weaker if observable at all. Interestingly, both fluorinated derivatives **2a** and **3a** show the strongest effects in their respective compound series; apparently, the proportion of the adduct in the equilibrium

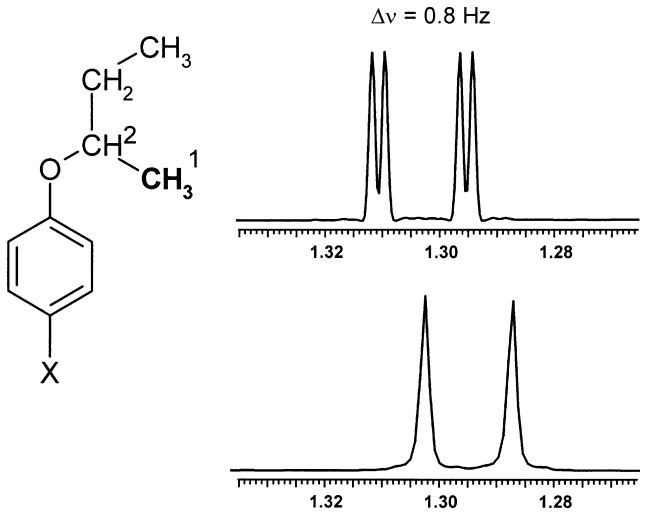

Figure 4. Signal dispersion $\Delta\nu$ of the H-1 signal of 1-fluoro-4(1-methylpropoxy)benzene (**2a**); bottom: free ligand, doublet due to ^{3}J(H-1,H-2); top: in the presence of one mole equivalent **Rh***.

(Scheme 4) is somewhat increased by fluorine so that splittings of the time-averaged NMR signals are less 'diluted'. This is in line with the above-mentioned observation that these two derivatives also show the strongest complexation shifts (see above). Both evidences support the enhancement of the oxygen donor properties by fluorine.

Some ^{1}H NMR signals display minute dispersions but this is basically confined to the fluorinated derivatives **2a** and **3a** again; see for example Fig. 4.

References

[1] (a) Boyar EB, Robinson SD. *Coord. Chem. Rev.* 1983; **50**: 109; (b) Cotton FA, Walton RA (eds). *Multiple Bonds between Metal Atoms* (2nd edn). Clarendon: Oxford, 1993.
[2] (a) Mertis C, Kravaritoy M, Chorianopoulou M, Koinis S, Psaroudakis N. *Top. Mol. Organ. Eng.* 1994; **11**: 321; (b)Doyle MP, McKervey MA, Ye T (eds). *Modern Catalytic Methods for Organic Synthesis with Diazo Compounds: From Cyclopropanes to Ylides*. Wiley: New York, 1998; (c) Endres A, Maas G. *Tetrahedron* 2002; **58**: 3999; (d) Nolan DT III, Singleton DA. *J. Am. Chem. Soc.* 2005; **127**: 6190 and references cited therein.
[3] Clarke MJ, Zhu F, Frasca DR. *Chem. Rev.* 1999; **99**: 2511.
[4] Duddeck H. *Chem. Rec.* 2005; **5**: 396 andreferences cited therein.
[5] Díaz-Gómez E, Brotin T, Duddeck H. *Tetrahedron: Asymmetry* 2007; **18**: 2155.
[6] Deubel DV. *Organometallics* 2002; **21**: 4303.
[7] Wypchlo K, Duddeck H. *Tetrahedron: Asymmetry* 1994; **5**: 27.
[8] Bergman J, Norrby P-O, Sand P. *Tetrahedron* 1990; **46**: 6113.
[9] Stavber S, Zupan M. *J. Chem. Soc., Chem. Commun.* 1981; 148.
[10] Hirano M, Yakabe S, Monobe H, Clark JH, Takashi M. *J. Chem. Soc., Perkin Trans. 1* 1997; 3081.
[11] Mori T, Inoue Y. *J. Phys. Chem. A* 2005; **109**: 2728.
[12] Takeuchi K, Sasaki M, Takatsu H. *Chem. Abstr.* 1987; **109**: 46346, Eur. Pat. Appl., 38EP 249933 A1 19871223.
[13] Paradisi C, Quintily U, Scorrano G. *J. Org. Chem.* 1983; **48**: 3022.
[14] Hirano M, Yakabe S, Monobe H, Morimoto T. *Can. J. Chem.* 1997; **75**: 1905.
[15] (a) Hundscheid FJA, Tandon VK, Rouwette PHFM, Van Leusen AM. *Tetrahedron* 1987; **43**: 5073; (b) Tandon VK, Singh KA, Rai S, Van Leusen AM. *Heterocycles* 2004; **64**: 347.
[16] (a) Ruddy SB, Mcintire GL, Roberts ME, Toner JL.*Chem. Abstr.* 1995; **124**: 127168; U.S. patent, 9, U.S. 5476646 A 19951219, cont.-in-part of U.S. 5,443,814; (b) Illig CR, Toner JL, Lee RW, Baker EJ. *Chem.*

Abstr. 1995; **123**: 250203; U.S. patent, 8, U.S. 5443814 A 19950822, cont.-in-part of U.S. 5,405,600.
[17] Ewing DF. *Org. Magn. Reson.* 1979; **12**: 499.
[18] Diaz Gómez E, Albert D, Duddeck H, Kozhushkov SI, de Meijere A. *Eur. J. Org. Chem.* 2006; 2278, equilibrium constants have been estimated from variable-temperature ^{1}H and ^{13}C NMR experiments conducted after publication.
[19] Exner O. In *Correlation Analysis in Chemistry*, Chapman NB, Shorter J (eds). Plenum Press: New York, London, 1978; 439.
[20] Density functional calculations (B3LYP 6–31G*) using SPARTAN 06 version 1.1.0, Wavefunction Inc., Irvine, CA 92612; see also: Shao Y, Molnar LF, Jung Y, Kussmann J, Ochsenfeld C, Brown ST, Gilbert ATB, Slipchenko LV, Levchenko SV, O'Neill DP, DiStasio Jr RA, Lochan RC, Wang T, Beran GJO, Besley NA, Herbert JM, Lin CY, Van Voorhis T, Chien SH, Sodt A, Steele RP, Rassolov VA, Maslen PE, Korambath PP, Adamson RD, Austin B, Baker J, Byrd EFC, Dachsel H, Doerksen RJ, Dreuw A, Dunietz BD, Dutoi AD, Furlani TR, Gwaltney SR, Heyden A, Hirata S, Hsu C-P, Kedziora G, Khalliulin RZ, Klunzinger P, Lee AM, Lee MS, Liang WZ, Lotan I, Nair N, Peters B, Proynov EI, Pieniazek PA, Rhee YM, Ritchie J, Rosta E, Sherrill CD, Simmonett AC, Subotnik JE, Woodcock HL III, Zhang W, Bell AT, Chakraborty AK, Chipman DM, Keil FJ, Warshel A, Hehre WJ, Schaefer HF, Kong J, Krylov AI, Gill PMW, Head-Gordon M. *Phys. Chem. Chem. Phys.* 2006; **8**: 3172.
[21] Karplus M, Pople JA. *J. Chem. Phys.* 1963; **38**: 2803.

